Integrated electrohydraulic control actuation system with centralized power plant for the Reusable Launch Vehicle Technology Demonstrator

V. Masilamani*, Manoj Kumar, S. Sankar Narayan, N. Raghu, M. N. Namboodiripad and T. Mookiah

Vikram Sarabhai Space Centre, Indian Space Research Organization, Thiruvananthapuram 695 022, India

An electrohydraulic control actuation system for actuating eight aerodynamic control surfaces of the two-stage technology demonstrator of the Indian reusable launch vehicle (RLV-TD) was developed, validated by extensive testing in various test beds, simulation runs and flight proven in the RLV-TD HEX-01 mission flight on 23 May 2016. A centralized hydraulic power generating unit (HPU) was used for powering the eight actuators located in two stages. The network of plumbings and control components of this actuation system were required to be laid out over the entire length and breadth of the vehicle measuring 17 m in length, to distribute the hydraulic power to all the actuators. The hydraulic actuation system had to work for the longest ever duration of 833 s for an Indian launch vehicle. Many challenges arose due to a single HPU for two stages, long complex network of plumbings, longest ever operating duration, thermal issues, second-stage structure resembling an aircraft, limited occupancy for operations at the launch pad, limited power source, etc. Necessary provisions were incorporated in the design to successfully overcome them. This article describes the development of the control actuation system.

Keywords: Aerodynamic control surfaces, control electronics, electrohydraulic actuation system, hydraulic power unit, servo design.

Introduction

DESIGN and realization of electrohydraulic actuation system for a scaled-down version of a non-conventional launch vehicle pose many technological challenges. An actuation system was developed for the technology demonstrator version of the Indian reusable launch vehicle (RLV-TD). The upper stage of the vehicle resembling an aircraft was mounted on a conventional cylindrical rocket stage. The launch vehicle had limited space. Many other systems also had to be accommodated in the fuselage. The vehicle had eight aerodynamic control surfaces located at aft end of the respective stages: four fins at the first stage base shroud for ascent flight control, and two elevons and two rudders in the winged second stage for descent flight control. The vehicle also had other control systems to control the vehicle during aerodynamic ineffective regimes. One actuator each deflected these eight control surfaces. Servo loops for the eight actuators were implemented in two units of control electronics for this purpose. All these eight control actuators located in two stages of the rocket were fed from a centralized hydraulic power unit located in the upper stage. A unique hydraulic line disconnect and sealing device specially developed indigenously by pyro system experts was employed for disconnecting and sealing the upper stage hydraulic circuit from the spent first stage hydraulic circuit at the end of burnout. Figure 1 shows the hydraulic scheme of the actuation system.

The prime mover and control components were located at different positions in the fuselage. The network of plumbings and control components laid out over the entire length of the vehicle measuring 17 m long used to distribute the hydraulic power to all actuators was complex. This was the longest ever operating hydraulic actuation system (60 s pre-flight + 773 s flight) for an Indian launch vehicle. The system was designed to absorb the heat generated in it within the system itself, without the need for any external cooling. A brushless direct current (BLDC) motor powered by lithium-ion battery was used as prime mover. The prime mover was switched 'on' 60 s before vehicle liftoff to allow the transients of BLDC motor and pump to settle, the pressures to stabilize and the free air, if any present, to dissolve in the fluid under pressure. The power was highly optimized to reduce the weight of the battery to be carried on-board.

There were many constraints due to the network of plumbing and components, flexibility requirements, thermal issues, plumbing natural frequencies, aircraft-like

*For correspondence. (e-mail: v_masilamani@vssc.gov.in)

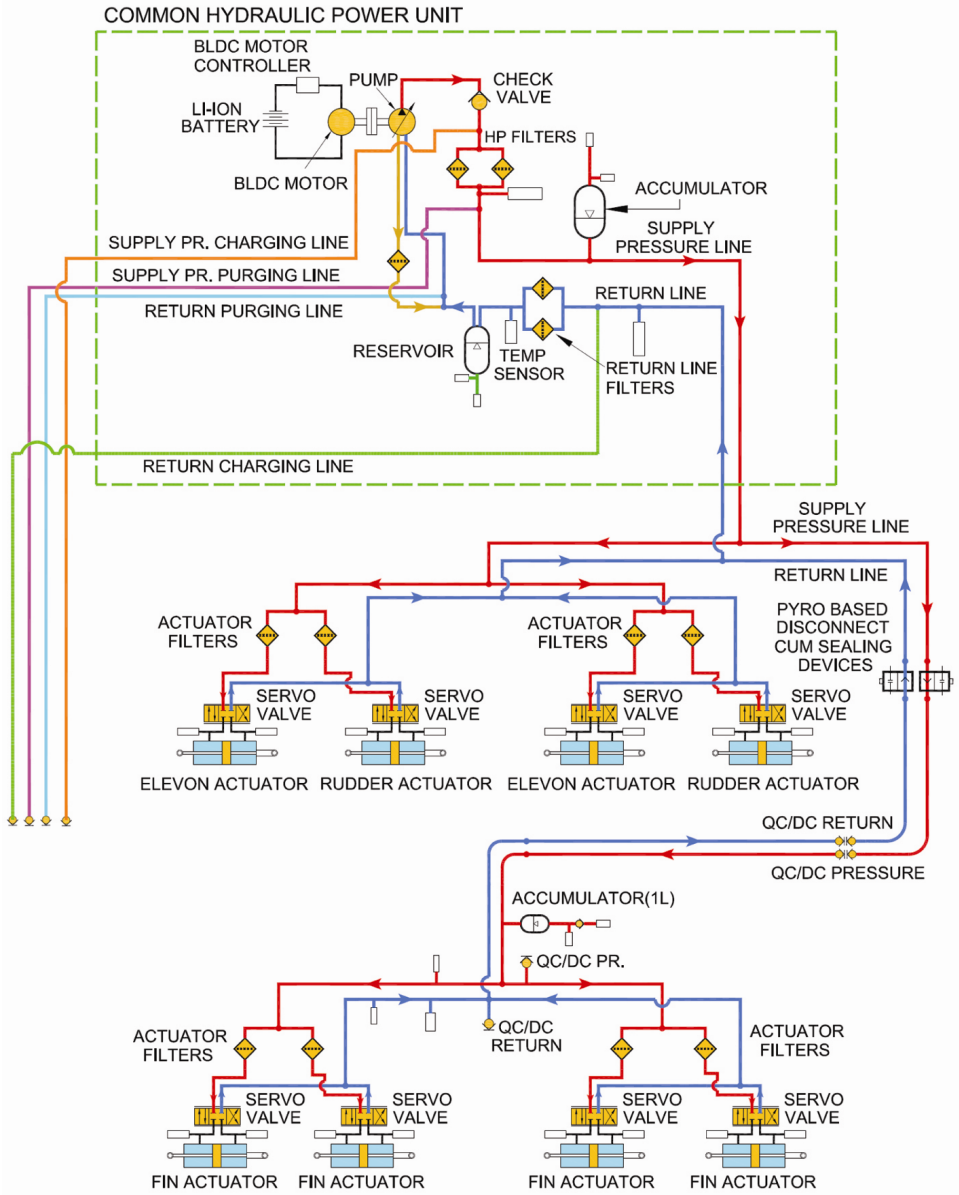

Figure 1. Hydraulic circuit of actuation system.

structure, limited occupancy for operations at launch pad, limited power source, etc. Preventive measures were taken to maintain system cleanliness better than class 6 of National Aerospace Standard (NAS) 1638, and also to keep the system free from entrapped and dissolved air. All the potential challenges were envisaged during the design phase itself, and provisions were incorporated in the design to successfully overcome them.

Description of the system and sizing of the control components and power plant

The system consisted of lithium-ion battery, high power controller for the BLDC motor, two units of control electronics each controlling four actuators, a BLDC motor, an axial piston pump with pressure compensator, a medium-sized accumulator to partially share the load on the pump, filters for contamination control, check valve, manifolds, eight actuators in all, several plumbing lines, a reservoir, and sensors for pressure, temperature and position feedback. The servo design consisted of a proportional integral type of compensator, a roll-off filter to take care of high frequency oscillations and a notch filter for the load resonant frequency. Electrohydarulic type of actuators (operating on 21 MPa supply pressure) were selected due to the continuous requirement of trim. In case of electromechanical actuators, to meet the continuous trim requirements, current needs to be continuously supplied to the actuators to keep the control surfaces in deflected condition, which would heat up the motor coils. The aerodynamic

Table 1. Control actuation system requirement specification and results achieved

Control actuation system parameter	Unit	Requirement specification	Achieved values (results of evaluation tests conducted on flight actuators)							
			Fin 1	Fin 2	Fin 3	Fin 4	Elevon 1	Elevon 2	Rudder 1	Rudder 2
5% Frequency response										
Bandwidth	Hz									
–3 dB gain		$6.5^{\pm 0.5}$	6.6	6.4	6.42	6.45	6.42	6.44	7.34	7.21
–90° phase		$7^{\pm 0.5}$	7.03	7.14	7.15	7.17	7.42	7.26	8.18	8.23
5% Step response										
Rise time	ms	$50^{\pm 10}$	47	6.08	51	51	41	47	41	44
Overshoot	%	≤25	9.35		5.6	5.75	12.79	11.94	10.69	11.08
Settling time	ms	<600	352	276	299	248	450	332	367	337

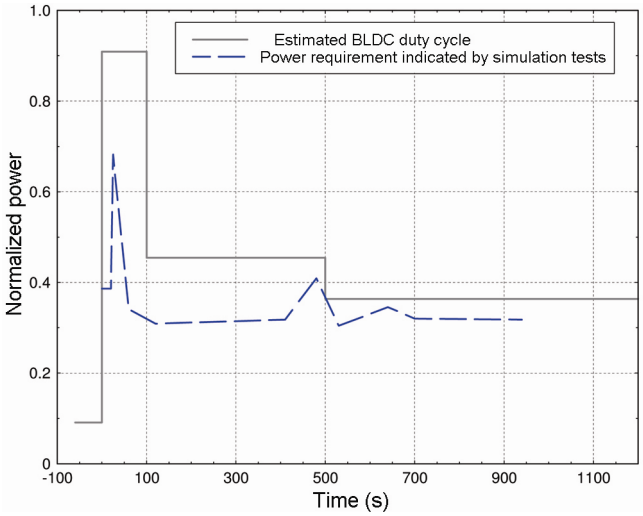

Figure 2. Control power plant (CPP) power demand indicated by 6D simulation run in the very early phase of the project.

hinge moments estimated by the aerodynamic experts were 1650 Nm on each of the two elevons in the second stage of the vehicle and each of the four fins on the first stage and 640 Nm on each of the two rudders in the second stage. Accounting for loads due to inertia of the moving parts, damping, friction, etc. the elevon and fin actuators were designed to deliver 1940 Nm minimum and the rudder actuators 1330 Nm minimum. The deflection requirement for all the control surfaces was 30° on either direction to meet the trim and control requirements. The bandwidth and load velocity requirements estimated by the digital auto pilot experts were 6.5 Hz and 60°/s respectively, for all the control surfaces. Table 1 gives the requirement specification for the actuation system and the results achieved.

The primary load on the actuators was the aerodynamic load (hinge moment) on the control surfaces. The other minor loads on the actuators were due to inertia of the control surfaces and friction in the bearings and seals. The actuators sizing was done as usual considering the hinge moments, inertia and friction loads, supply pressure and pressure drop in the servo valve[1]. For the given hinge moment and chosen supply pressure, an actuator was designed in-house. For standardization and variety reduction, all the eight actuators were of the same area and stroke.

The servo valve selection was done using load locus and valve capability curves for the chosen supply pressure and arm lengths, considering inclination effects due to deflection of control surfaces[1].

The power rating of the control power plant (CPP) is normally decided by the load and load velocity requirements. In this particular case, the main objective was to optimize the power requirement to the maximum extent possible. The battery size and weight had to be small. Conventional design approach would have demanded four times the power that was actually provided. However, this was in no way affordable considering the size of the vehicle and allotted mass budget of the control actuation system. To minimize the power requirement, the following strategies were adapted and the CPP power was finalized.

(1) The load velocity would be based on reduced amplitude (5%) rather than the conventional 10% of the full deflection range of the control surfaces. This was decided mainly based on the initial simulations conducted.

(2) Half of the peak power would be shared by a suitably sized accumulator. However, the duration of each demand from the accumulator would be limited to protect the actuator force capability.

Extensive simulation runs were carried out by the task team in the very early phase of the project with the then available input to confirm the adequacy of the power plant size. Figure 2 shows the cumulative power demand (at the output shaft of the prime mover) as indicated by the simulation run and the estimated peak power and duty cycle for the BLDC motor.

Figure 3 shows the power demand during flight (at the output shaft of the prime mover). The peak power and duty cycle demanded by the flight are within the estimated

requirements. The power demand from 115 to 215 s of flight is due to higher command on the elevon actuators.

An accumulator was developed to provide half of the hydraulic power. After extensive simulation studies, it was decided that such an additional demand would last less than 2 s each. This is to minimize the accumulator size and still maintain the system supply pressures within acceptable levels for protecting the actuator force capability. A piston-type hydro-pneumatic accumulator was designed based on the discharge rate required from the accumulator, duration of each such discharge, supply pressure and the lower bound of actuator force capability[1]. In piston-type designs, dilation of the cylinder due to internal pressure can cause gas leakage across the piston seal. Also, the length of the accumulator had to be limited to accommodate it within the smaller available envelope. For these reasons, two concentric shells configuration was chosen for the accumulator. This configuration will not cause dilation of the inner cylinder, as there is no differential pressure between the inner and outer surfaces of the inner cylinder. Figure 4 shows the schematic diagram of the newly developed accumulator.

Several ingenious techniques were used during the course of development of this accumulator. The first one being the usage of three proprietary piston seals on the piston to avoid degradation of the seals due to simultaneous exposure to gaseous and oil media. In this design, one seal is exposed only to gas medium, the other seal is exposed only to oil medium and the middle seal, which is the main seal, is not exposed to any medium, but only to oil traces. This ensured longest ever leak-free wet life for the accumulator. The second technique being the special mounting scheme designed to accommodate the axial expansion and radial dilation (caused by the internal pressure and oil temperature) of the accumulator. This mounting scheme with 'one end fixed – other end free' configuration is explained later in the text. In the third technique, to take care of the axial expansion of the inner cylinder and prevent compressive load and consequent bulging, a shim was used between the gas side cover and outer shell. This created the necessary gap for the inner cylinder to axially expand due to oil temperature rise. The oil in the accumulator was additionally used as a thermal mass to contain the system oil temperature. Further details are given later in the text.

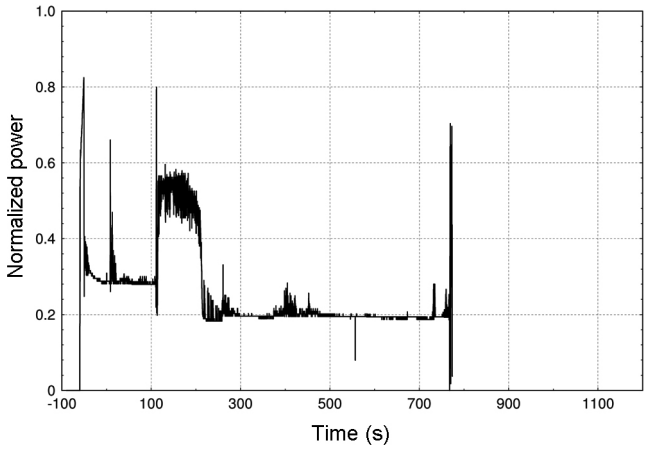

Figure 3. CPP power demand during flight.

Reservoir capacity was decided based on accumulator size and pump discharge[1]. The reservoir was also made of two concentric shells configuration to avoid across-piston seal leakage due to dilation. The reservoir was mounted using the same 'one end fixed–other end free' scheme. Here also, a shim was used to take care of axial expansion of the inner shell. The oil contained in the reservoir was also used as a thermal mass to contain the system oil temperature. Figure 5 shows the schematic diagram of the reservoir.

The discharge rate and operating speed of the pump were decided based on the cross-section of the actuators, load velocity requirements and accumulator capability. An already developed pump was chosen and operated at higher speed after due qualification testing, to minimize the system development time.

A BLDC motor was developed as the prime mover. The specification of the BLDC motor was finalized based on the system operating pressure and discharge of the pump, and expected duty cycle of the system derived from simulation studies. The BLDC motor was operated using a high power control electronics in open loop as the lithium-ion battery voltage was fairly stable for the duty cycle and operating duration. The in-rush current during switch 'on' was limited by a soft start circuit in the control electronics (CE) in order to avoid battery discharge and protect switching devices in the CE. The BLDC motor–pump transient was expected to take about 20 s to settle down. Hence, the motor was switched on 60 s before vehicle liftoff.

Challenges encountered during system development and mitigation

Many challenges were faced during development of the actuation system. These were due to the following: (1) The vehicle being a technology demonstrator was a scaled-down version with limited space. (2) The upper stage was a winged body with its structure resembling the aircraft fuselage. (3) The system had the longest ever hydraulic plumbing network distributed over about 17 m length. (4) There was no space in the first stage base shroud for accommodating a hydraulic power generating unit (HPU). Therefore, the actuation systems of both the stages were provided with only one centralized HPU located at the second stage. This was possible because the power demanded by the actuation systems of both the stages was fairly equal. A few of the challenges faced are described below.

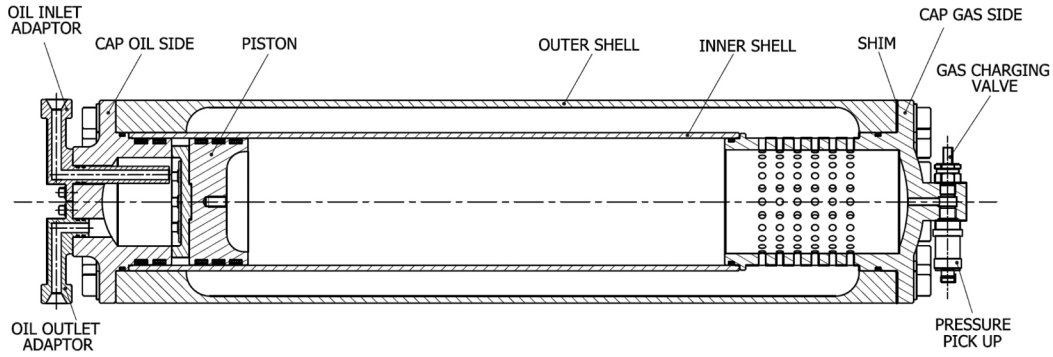

Figure 4. Accumulator.

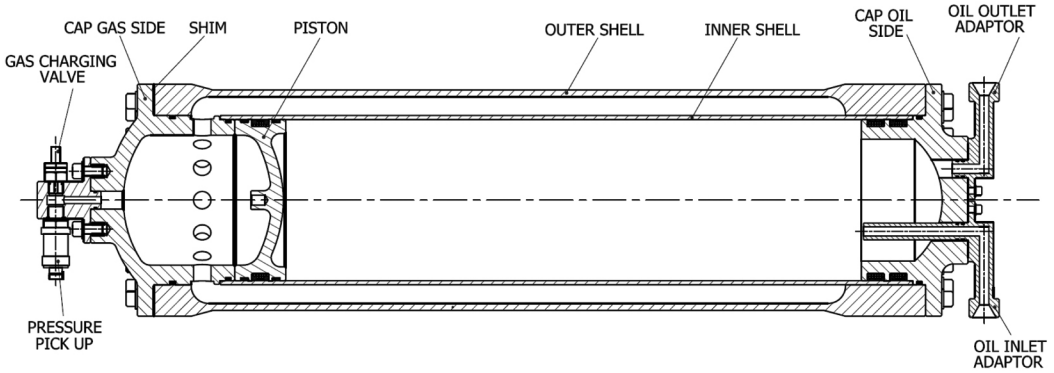

Figure 5. Reservoir.

Thermal challenges

Oil temperature rise: The rise in oil temperature would lead to oil leakage through the plumbing joints, jamming of accumulator and reservoir pistons, axial expansion of accumulator and reservoir shells, axial expansion of tubes, thermal expansion of oil and consequent rise in return line pressure, separation of air from the oil, etc. Based on experience, it was decided to limit the oil temperature below 75°C. The hydraulic system oil temperature rises due to internal heating caused by: (a) Power loss in the servo valves (during power transfer and internal leakage). (b) Pump inefficiencies (mechanical and volumetric). (c) Actuator friction power (due to seal friction). (d) Hydraulic line losses (due to friction, variation in cross-section and direction, etc.)

The expected rise in the oil temperature was estimated with following assumptions. (a) Power loss due to air in the oil (lower bulk modulus) is negligible. (b) Heat is contained within the metal and oil of the actuation system, and not transferred to surrounding air and structures by radiation, convection and conduction. (c) Specific heat (C_p) for Mil-PRF-5606 oil is 1.97 kJ/kg K and for steel is 0.46 kJ/kg K. (d) There is no external heat load on the actuation system due to aerodynamic heating, conduction through structures and radiation. (e) Temperature rise is estimated assuming steady-state conditions. (f) Total operating duration for the system is taken as 860 s (60 s pre-flight, 110 s ascent flight and 690 s descent flight) for the purpose of heat estimation.

The mass of metal and oil contained in the system during ascent and return flights was estimated.

The optimistic estimate (with the assumption that the metallic materials of the actuation system also serve as a heat sink) gave the oil temperature rise (ΔT) for 860 s duration as 22°C over the ambient. The pessimistic estimate (assuming that the oil only absorbs the heat) gave the temperature rise (ΔT) as 78°C over the ambient.

To get an initial feel of the overall system performance and oil temperature rise, a laboratory-level initial system testing was conducted. To minimize the development time and cost, this test was done without simulating the plumbing lengths, manifolds, filters and hoses, etc. During this initial test, the oil temperature rose rapidly. It rose by 47°C (ΔT) in 720 s (Figure 6). The pump temperature rose by 55°C (ΔT) in 720 s. The oil started to seep out from the plumbing joints, indicating the beginning of lack of sealing due to lower viscosity and thermal effects on the plumbing lines.

As seen in Figure 6, the reason for this is the oil in the accumulator and reservoir did not absorb heat. The accumulator and reservoir had only one port for the oil to enter and exit. This was rectified by modifying the accumulator and reservoir so that the oil forcibly enters,

mixes with the cooler oil inside and then comes out. This modification brought down the oil temperature to acceptable levels. An Iron Bird test rig which was exclusively developed for simulation studies with flight equivalent actuation system hardware was used for extensive testing of the actuation system. Hundreds of simulation tests were carried out on the actuation system using this test rig to evaluate many cases with different objectives. During all of these tests, the rise in oil temperature was within acceptable limits. Figure 7 shows the oil temperature rise during few of the sample cases of simulation tests (on the actuation system in the Iron Bird test rig) after the above-mentioned modification in accumulator and reservoir.

The flight telemetry data indicate that the oil temperature rise for a duration of 833 s (60 s pre-flight + 773 s flight) matches with the optimistic estimate (Figure 8).

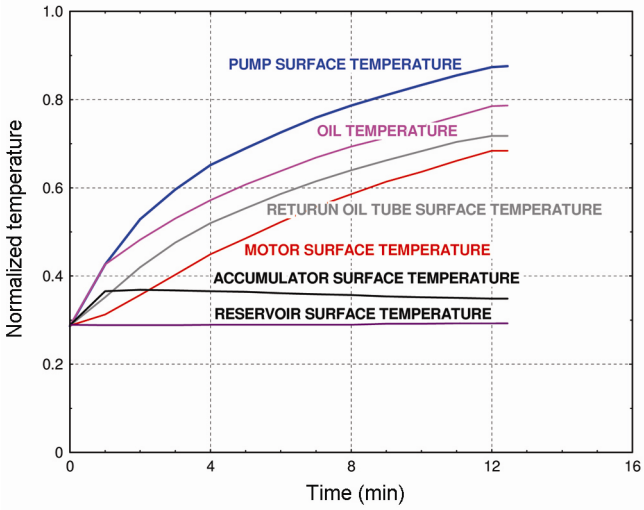

Figure 6. Laboratory-level system testing showing abnormal oil temperature rise.

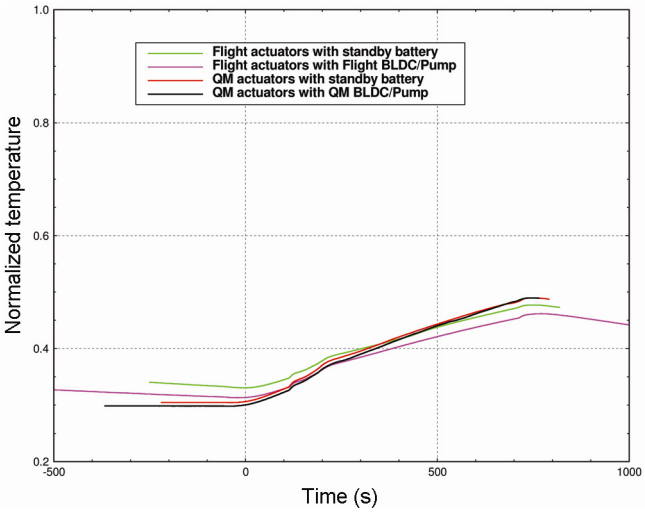

Figure 7. Oil temperature rise during various simulation runs on Iron Bird test rig.

Thermal expansion-related challenges in accumulator and reservoir: (i) Accumulator and reservoir mounting to fuselage – Accumulator and reservoir were of piston type and of two concentric shells configuration. The outer shell would axially expand both due to internal pressure and oil temperature rise. The internal shell would expand due to oil temperature rise. The inner shell containing the oil would expand first. The estimated axial expansion (for an oil temperature rise of $\Delta T = 78°C$) of the accumulator outer shell: 0.1 mm due to pressure, 0.5 mm due to thermal expansion and total axial expansion 0.6 mm. Reservoir outer shell expansion: 0.012 mm due to pressure, 1.2 mm due to thermal expansion and total axial expansion = 1.212 mm.

Figure 9 shows the 'one end fixed and the other end free' mounting configuration specially designed for accumulator and reservoir. As shown in the figure, the accumulator and reservoir are supported on two saddle-type aluminium alloy brackets firmly bolted to the fuselage. The shells are mounted to these support brackets using 15-5 PH stainless steel 'fork and tongue'-type holding brackets at the free end. The forks are fixed to the support bracket, while the tongues are fixed to the shells. The forks have a cylindrical hole and the tongue is provided with an elliptical hole. A cylindrical pin is inserted using sliding fit into the fork and tongue resulting in the required amount of gap at the aft portion of the tongue. As shown in Figure 9, the shell carrying the tongue can expand. At the fixed end, single piece 15-5 PH stainless steel brackets are used. This mounting configuration has been realized and tested in the laboratory up to 75°C temperature. Tests have also been conducted multiple times in the Iron Bird test rig during simulation runs.

(ii) Managing inner shell expansion – The oil would transfer the heat to the inner shell. The inner shell would expand first before the outer shell feels the heat. This

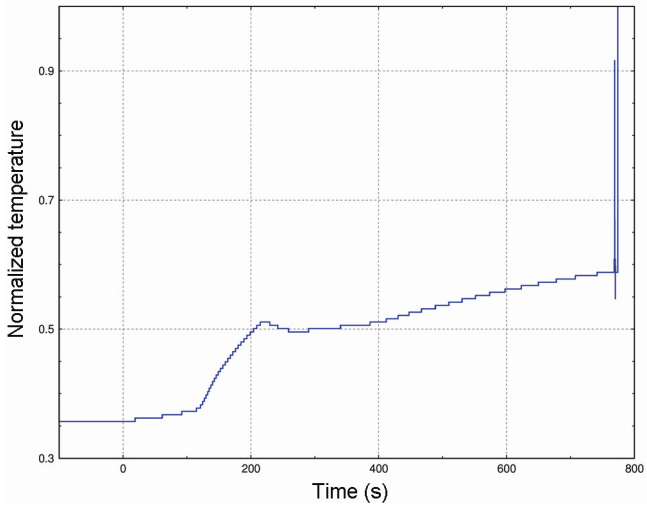

Figure 8. Oil temperature rise during flight.

expansion, if not managed, would result in compressive loads on the inner shell leading to bulging. Such a bulging would lead to loss of sealing force and the gas would leak across the piston leading to failure. The estimated axial expansions for the inner shells of the accumulator and reservoir were 125 and 145 µm respectively. To prevent this type of failure, shims of 500 µm thickness were introduced at the gas side of the accumulator and reservoir between the gas side cover and outer shell resulting in the required amount of gap between the mechanical stopper on the gas side cover and the inner shell.

(iii) Prevention of jamming of piston inside the inner shell – The pistons of the accumulator and reservoir were made of aluminium alloy to minimize their mass. The inner shells were made of 15-5 PH stainless steel (for fabrication purposes to achieve the required surface hardness, surface finish for the seals to slide inside, wear

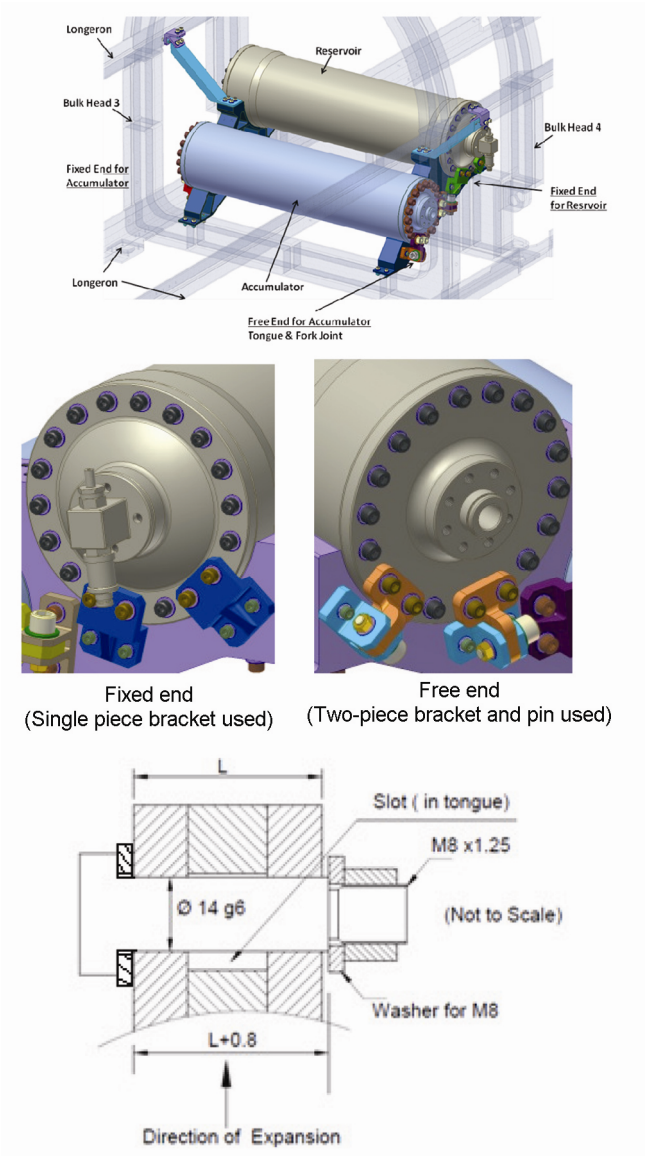

Figure 9. One end fixed and the other end free mounting configuration of accumulator and reservoir.

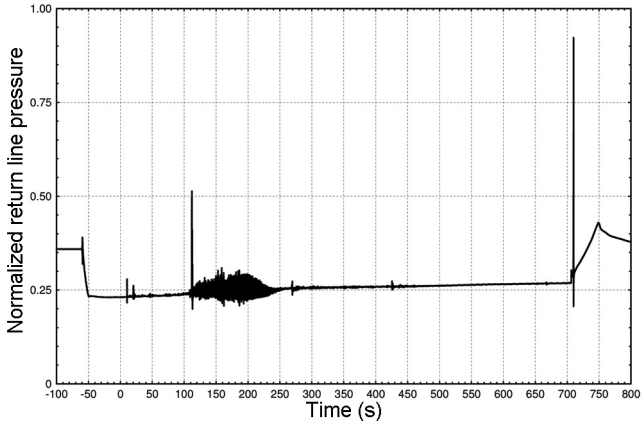

Figure 10. Return line pressure increase during simulation test.

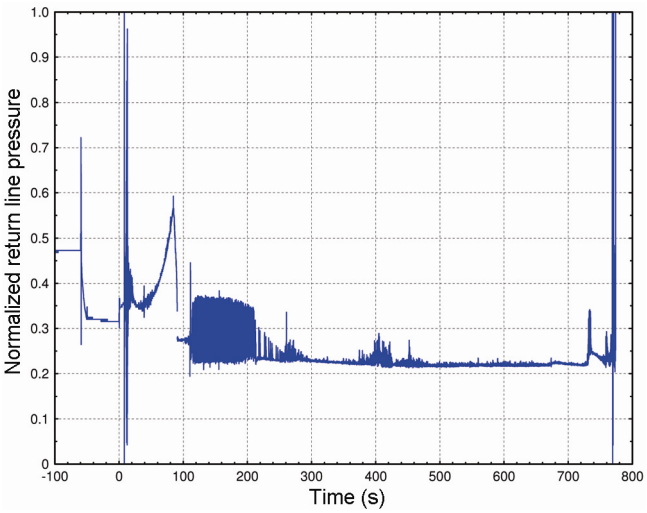

Figure 11. Return line pressure in flight.

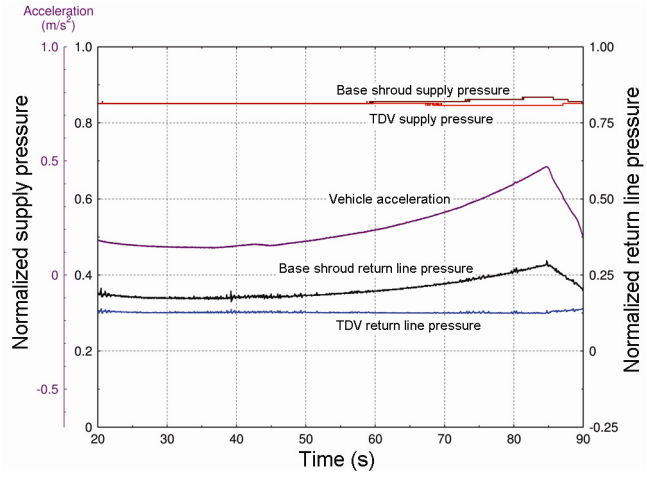

Figure 12. Gradual rise in base shroud return line pressure due to the effect of vehicle acceleration on the column of hydraulic fluid.

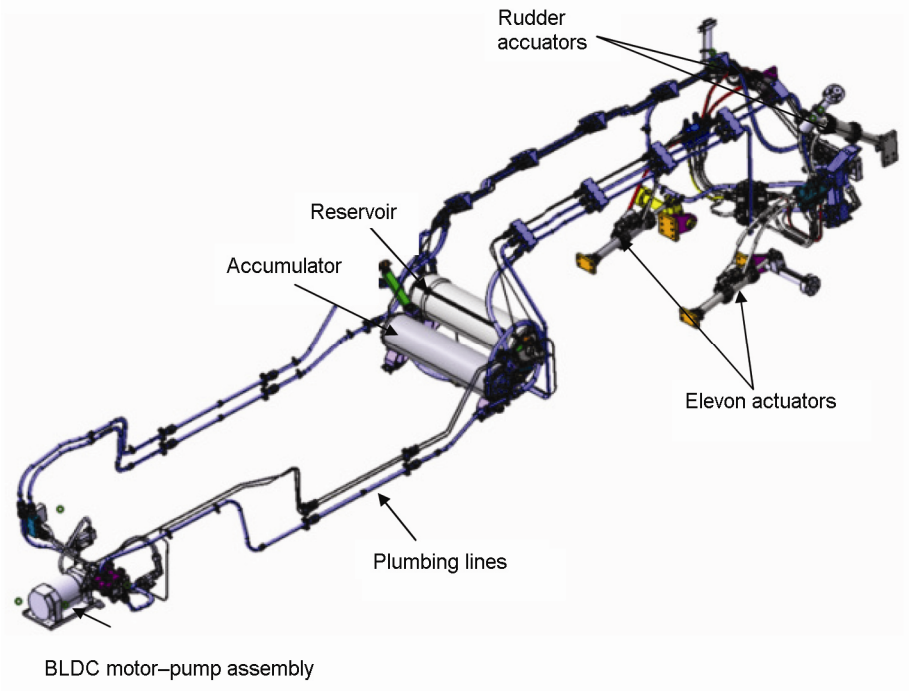

Figure 13. Plumbing layout in second stage.

resistance, rigidity, etc.). As the temperature rises, the aluminium piston would expand approximately at twice the rate of the steel inner shell, resulting in jamming of the piston and failure of the accumulator and reservoir. The estimated decrease in diametric clearances were 29 and 37 μm respectively, for the accumulator and reservoir for the optimistic temperature rise of 22°C and 101 and 130 μm respectively for the pessimistic temperature rise of 78°C. Providing a higher diametral clearance to account for a higher temperature rise would lead to less sealing force since the oil is initially at ambient temperature and also the piston will have tilting tendency. Based on the oil temperature rise noticed during the extensive laboratory and simulation tests, jamming of the piston inside the inner cylinder was prevented by appropriately sizing the seal groove, outer diameter of the piston and bore of the inner shell.

Effect of oil temperature rise on return line pressure: The increase in oil temperature by 22°C would heat up the gas in the accumulator and reservoir. For this size of accumulator and reservoir, the notional volume increase expected in the accumulator gas was around 7%. This would gradually push about 0.3 litres of oil into the return line. Similarly, the notional increase in reservoir gas is 0.64 litres. The thermal expansion of oil would amount to 0.23 litres. The total volume is 1.17 litres. This would increase the return line pressure by 0.07 MPa. Such an increase in return line pressure was noticed during actuator in loop simulation (ALS) tests on Iron Bird test rig (Figure 10). However, such an increase was not noticed in the flight as shown in the return line pressure plot in Figure 11, for the entire duration of the flight. This plot is a combination of return line pressure of first stage up to the end of first stage flight and second stage return line pressure from the end of first stage flight to end of the flight. This observation is probably due to the effect of vehicle deceleration from $T + 85$ s (the vehicle was accelerating up to $T + 85$s and decelerating thereafter). However, a gradual pressure rise of 0.685 MPa in the first stage return line pressure and 0.4 MPa in the first stage supply pressure lasting up to $T + 85$ s of the flight was noticed during the ascent flight. This was due to vehicle acceleration and mass of fluid column (Figure 12). Since the return line of the system was also designed for an operating pressure rating equivalent to the supply pressure (to take care of pressure surges or water hammer due to sudden deceleration of oil in the long plumbing lines, to foolproof the components from human error during testing and also standardize them for variety reduction), there was no concern.

Thermal expansion of plumbing lines: Figures 13–15 show the plumbing lines consisting of tubes and hoses. To take care of thermal expansion of tubes in plumbing lines, special bulk head joints were designed (Figures 16 and 17). Figure 16 shows the type of bulk head joint used for 20 mm outer diameter tubes. Here also 'fixed–free' mounting configuration was adopted to take care of thermal expansion of the tubes. Each tube segment had one fixed end using a 37° flare connection and a free-floating end with radial seals (shaft seals). Figure 17 shows the

type of bulk head joint used for 4.7 mm diameter tubes. Each tube piece had one fixed end using an axial seal (face seal) and swivel nut connection and a free-floating end with shaft seals. In both cases, in the free-floating ends, the required amount of gap was provided in front of the unions attached to the tubes after estimating the thermal expansion for the length of the tube used.

Tubes of 10 m length were required to be laid over the first stage motor case because of the centralized power plant scheme for conveying the hydraulic power from the second stage to the first stage base shroud. Figure 15 shows the configuration of the plumbing lines used over the motor case. To take care of the motor case axial expansion (due to temperature rise and pressure), these tubes were provided with a fixed joint at the middle and sliding joints (using PTFE bushes) at 34 locations to allow free movement when the motor case expands. Figure 15 also shows the configuration of specially designed fixed joint at middle and sliding joints. Further, the tubes were connected at both ends to the stages using flexible hoses which will stretch and accommodate the motor case expansion.

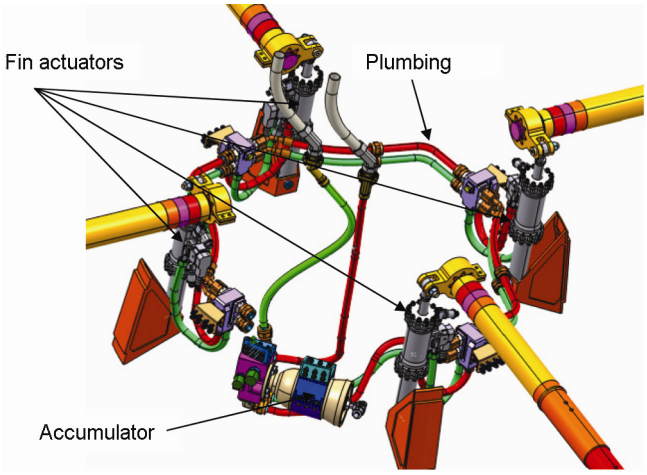

Figure 14. Plumbing layout in first stage base shroud.

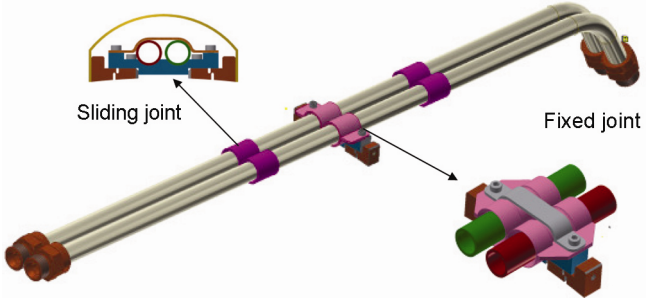

Figure 15. Plumbing layout on first stage motor case.

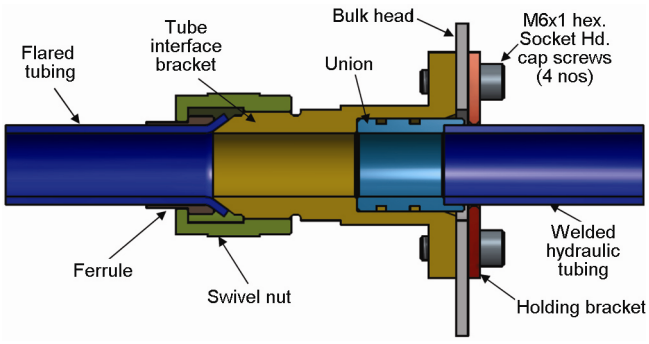

Figure 16. Bulk head joint for higher diameter tubes.

Structural requirements of plumbing lines

As shown in Figures 1 and 13–15, the plumbing lines consisting of tubes and hoses had to be laid over the entire length of the vehicle due to its aircraft-like configuration and locations of aerodynamic control surfaces, control components and actuators. Since these plumbing lines have to coexist with other mechanical, electrical, avionics, pyro systems, etc. they should be leak-free. We need to take care of the potential failure modes of the plumbing. All the plumbing lines were analysed by structural experts for assessment of expansion at the joints and stresses on tubes due to internal pressure, temperature

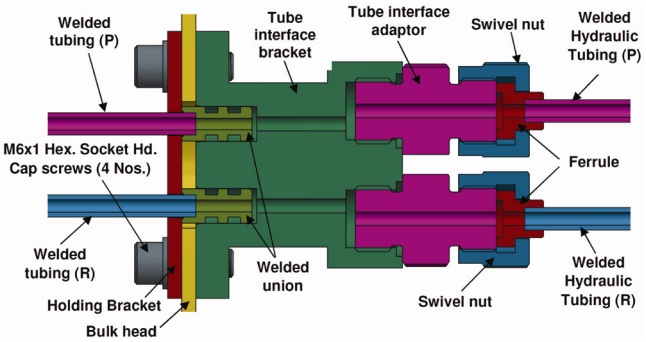

Figure 17. Bulk head joint for smaller diameter tubes.

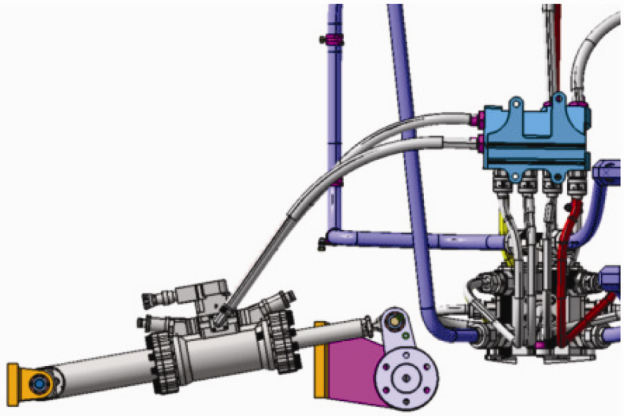

Figure 18. Hoses at the pressure and return ports of the actuator.

and structural deformation by finite element modelling and analysis. All the tubes were clamped using loop-type rubber cushioned clamps to achieve the natural frequencies above the required value. The tube natural frequencies were measured by tap tests. The plumbing consisting of a combination of tubes and hoses was also subjected to tap tests.

Flexibility provisions were made in the plumbing lines and components as given below.

Hoses for pump ports: The BLDC motor–pump operation would generate self-induced vibrations. To take care of this, the suction, delivery and case drain lines were provided with hoses.

Accumulator and reservoir: The accumulator and reservoir would expand due to internal pressure and oil temperature rise. The estimated axial expansions (for pessimistic estimate of oil temperature rise $\Delta T = 78°C$) were 0.6 mm for the accumulator and 1.212 mm for the reservoir, as explained earlier in the text.

The inlet and outlet lines of the accumulator and reservoir were connected to the plumbing lines using hoses to take care of the axial expansion. The accumulator and reservoir were mounted to the fuselage using specially designed tongue and fork joints. This provided 1 mm expansion gap for the accumulator and 2 mm expansion gap for the reservoir. Figure 9 provides the details.

Actuators: The estimated sway of actuators due to deflection of the control surfaces by ±30° is given below.

Booster fin actuators of first stage: ± 8°20′.
Rudder actuators of second stage: ± 5°13′
Elevon actuators of second stage: ± 7°28′.

Hoses were used to connect the pressure and return lines with the system to take care of sway during actuation (Figure 18).

Plumbing in Technology Demonstrator Vehicle (TDV): Thermal expansion would increase the length of tube segments used in the plumbing. A gap of 1.5 mm gap was provided to take care of thermal expansion in front of the unions attached to each tube segments (Figures 16 and 17).

Inter stage: The hydraulic power from the upper stage was conveyed to the first stage using hoses at the inter stage region (Figure 19). These hoses also provided the necessary flexibility for their ejection during disconnection and sealing of the hydraulic lines. Quick connect disconnect couplings (QCDCs) were provided in these hoses for connecting the oil-charged stages at the launch pad. This provision of QCDCs was made to do away with the requirement of oil charging the actuation system at launch pad.

Actuation system plumbing laid over first stage rocket motor case: Estimated axial expansion of first stage rocket motor case was 11 mm (7.5 mm due to temperature rise and 3.5 mm due to pressure). Details of the provisions made in the plumbing to take care this expansion are given in Figure 15, and explained in the preceding section.

Plumbing in first stage base shroud: To take care of the deflections and vibrations in the first stage base shroud, the pressure and return lines were made of combinations of tubes and hoses (Figure 20). The first stage actuator pressure and return lines were also connected to the plumbing lines by hoses to take care of the sway during deflection of the fins.

Prevention of water hammer effects due to greater lengths of plumbing lines

The plumbing lines were long. The power plant was 17 m away from the four first-stage actuators. As shown in Figures 1 and 13–15, the plumbing lines consisting of tubes and hoses had to be laid over the entire length of the vehicle. There were hydraulic line disconnect and sealing devices on each of the pressure and return lines. These devices close the lines instantly under pressure and flow.

The accumulator in the second stage and a small accumulator provided in the first stage would prevent water

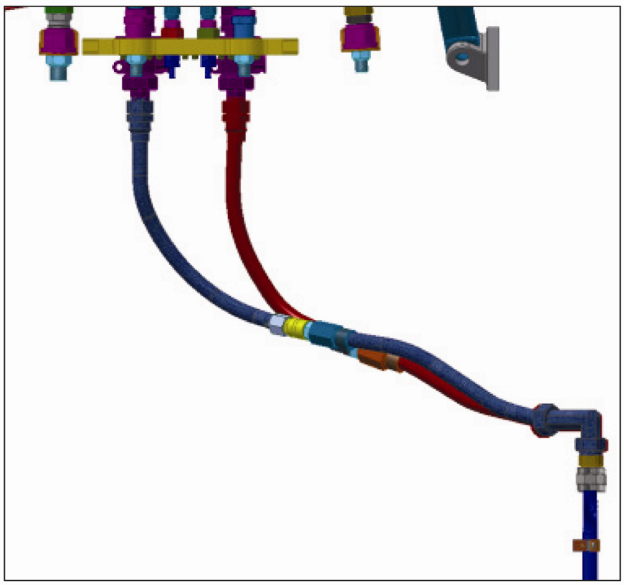

Figure 19. Hoses of the pressure and return lines in the inter-stage region.

hammer effects in the supply pressure line. The reservoir provided in the second stage would prevent water hammer effects in the return line. No reservoir was provided in the first-stage return line. However, the entire return line up to the pump suction was rated for a higher operating pressure equivalent to the supply pressure as explained earlier.

The pressure rise due to sudden closure was analysed. For the estimated oil flow rate and line size, the flow velocity was 2 m/s. Assuming that the accumulator and reservoir are not present, the notional pressure rise in case of instantaneous closure was estimated[1]. Assuming the mass density for oil as 870 kg/m^3 and the sound velocity in oil as 890 m/s, for 2 m/s flow velocity the pressure rise would be 1.54 MPa. For 10 m line lengths, the frequency of such pressure waves would be 44.5 Hz. To nullify this effect, only about 5 ml of oil needs to be absorbed[1] in the accumulator (assuming 10 m line length and 0.69 GPa effective bulk modulus for the oil). The accumulators and reservoir functioned effectively in the flight and as can be seen from Figure 21, no such water hammer effects occurred.

However, during ascent flight, there was a pressure transient of magnitude about 1.5 MPa at 1 Hz rate in the return line pressure of the system (Figures 22 and 23). This happened at $T + 8.2$ s during the ascent flight control capture by the first-stage actuation system. As is evident from Figure 24, all the four first-stage actuators received commands simultaneously at maximum of designed rates at this instant. Momentarily, this demand was being met by the nearby first-stage accumulator (Figure 23). The pump (located at the second stage) was till then discharging equal to the null leakage of the actuators. It was drawing oil from the suction line at a rate equal to the null leakage of the actuators. At $T + 8.2$ s, due to the simultaneous commands, all the four first-stage actuators started discharging into the return line. The pump located in the second stage was yet to feel the demand at that moment and respond. The transient observed in the return line pressure was due to the above reason. Since the return line was also designed for a pressure rating equal to the supply pressure, there was no concern. In the flight, no relief valve was provided in the circuit either in the pressure line or in the return line. However, during simulation tests in the Iron Bird test rig, a relief valve was provided in the return line as a safety measure.

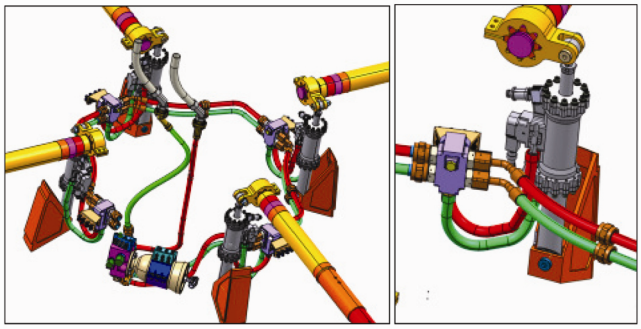

Figure 20. Base shroud pressure and return lines made using combinations of tubes and hoses.

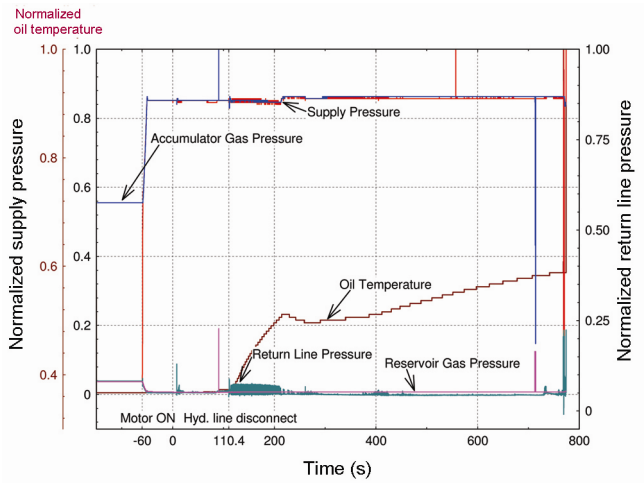

Figure 21. System pressures for the entire flight duration.

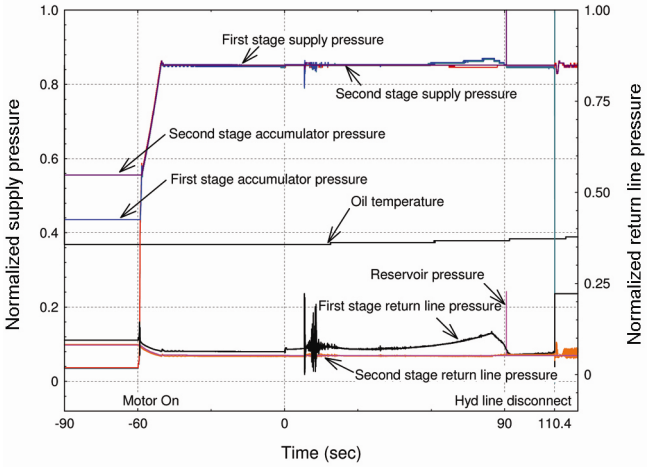

Figure 22. System pressures during first-stage flight.

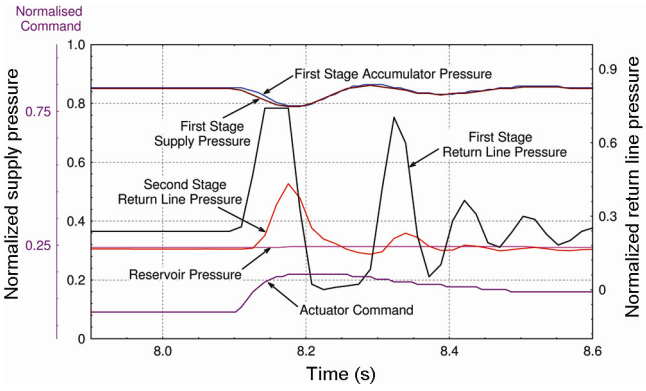

Figure 23. Pressure transient in system return line pressure during first-stage flight.

Sealing and disconnection of hydraulic lines

As explained earlier, a centralized power plant located at the second stage was used for the first time for powering the electrohydraulic actuation systems of two stages of a rocket. This necessitated a device which will disconnect the hydraulic lines at the end of burnout of the first stage and simultaneously seal the upper stage hydraulic supply pressure and return lines without any loss of fluid. This disconnection and sealing has to take place under the respective operating pressures of supply pressure and return lines. A unique device was specially developed by the in-house pyro experts highly specialized in the field. The device underwent a formal qualification programme. After laboratory-level tests, the device was successfully used in this mission for the first time. The disconnection occurred at $T + 110.4$ s. The system pressures were perfectly maintained without any loss of fluid from the upper stage (Figure 21). This shows the perfect functioning of the devices mounted both on supply pressure and return lines.

System cleanliness and prevention of aeration

Preventive measures were taken to maintain system cleanliness better than class-6 level specified in the National Aerospace Standard (NAS) 1638 and to keep the system free from entrapped and dissolved air. The following steps were taken during preparation, assembly, integration, oil charging and testing operations.

(1) Pre-cleaning of all components (vapour degreasing and solvent cleaning) before assembly.

(2) Flushing of the tubes and hoses before assembly with clean oil under pressure till better than NAS cleanliness class 6 is achieved consecutively three times.

(3) Flushing and purging of the system under low pressure first and then under high pressure with all actuators exercising sinusoidal commands of 90% amplitude at low frequency till better than NAS cleanliness class 6 is achieved consecutively three times.

(4) Oil charging with simultaneous purging of the system under pressure (to prevent entry of atmospheric air into the system) with fresh oil of better than NAS cleanliness class 3.

(5) Mating and de-mating of the two flight stages were performed under pressurized condition only to avoid the entry of atmospheric air into the system.

(6) Storage of the system in two flight stages under pressurized condition only.

(7) Adequate filters of suitable flow rating were provided in the system as listed below. Redundant filters were provided at critical locations like pressure line and return line. (a) Two numbers of 10 μm rated filters were provided in the pressure line (Figure 1). (b) Two numbers of 25 μm rated filters were provided in the return line. (c) Each actuator was provided with a 10 μm rated filter.

The system, with a complicated network of plumbings distributed over 17 m length with hundreds of joints, ten manifolds and eight actuators, underwent many pre-flight tests (close to 20,000 cycles for the actuators, and 65 starts for the pump and motor), but never showed any sign of aeration or contamination. The plot of system supply pressure during the flight was so steady (Figure 21), indicating that no air was present in the system. All

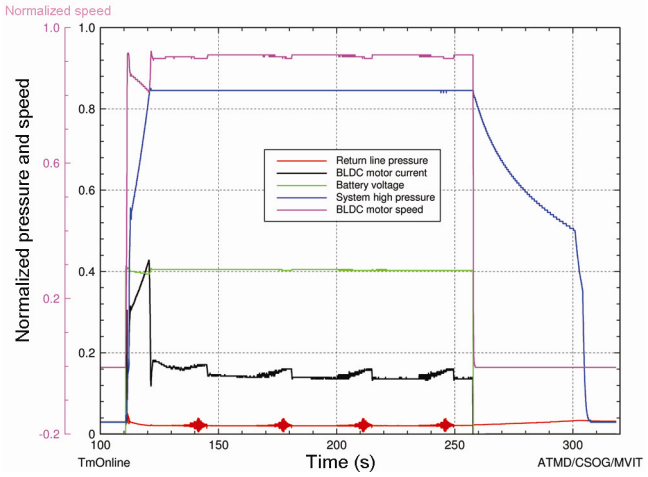

Figure 24. Performance of the hydraulic power plant during frequency response tests on first-stage actuators in full vehicle.

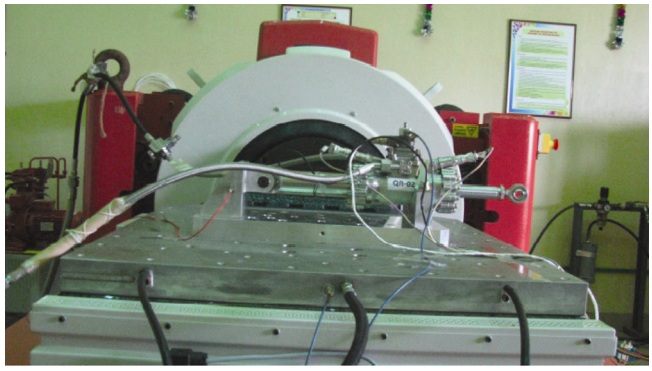

Figure 25. Actuator undergoing qualification vibration tests in active mode.

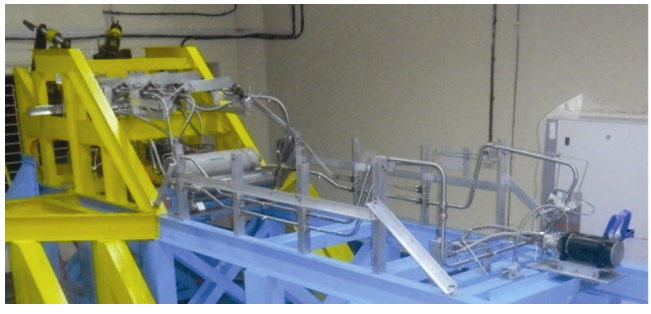

Figure 26. Iron Bird test rig for flight simulation runs with the actuation system in loop.

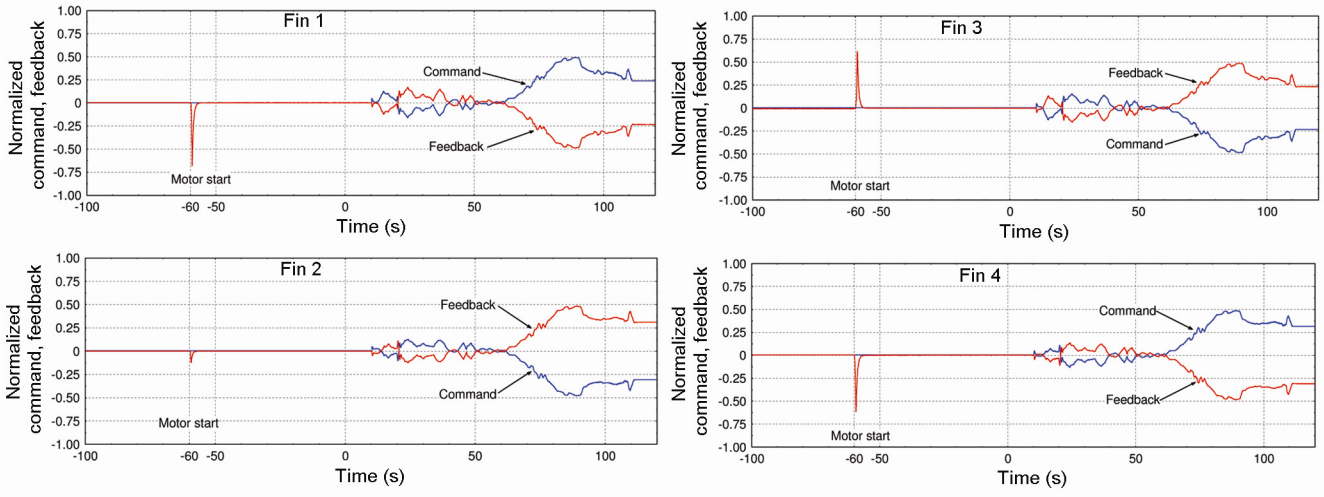

Figure 27. Results of nominal flight ALS run on first-stage actuators for deflecting fins.

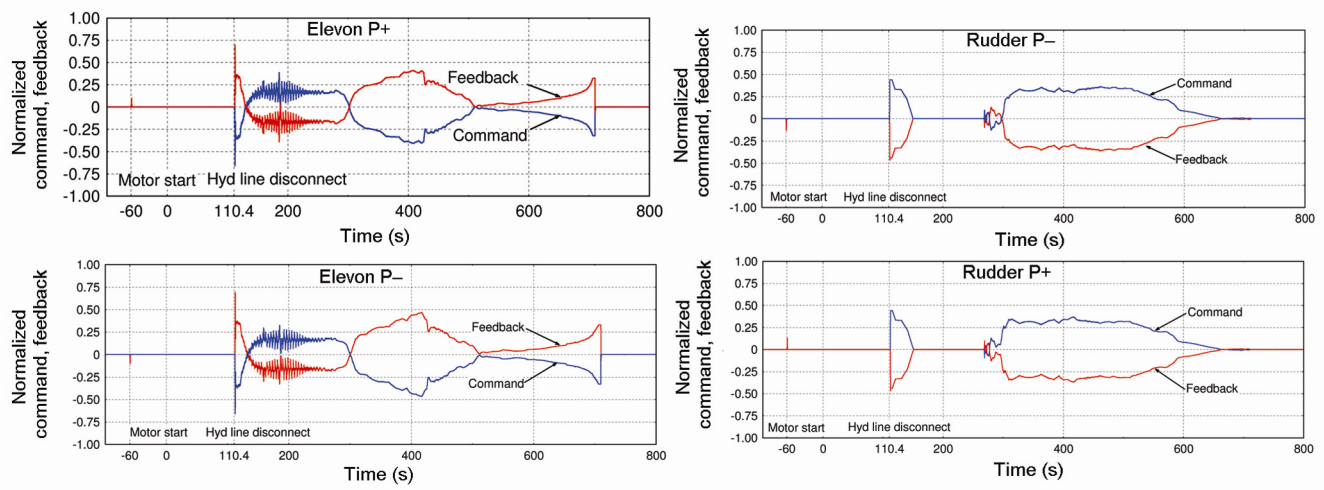

Figure 28. Results of nominal flight ALS run on second-stage actuators for deflecting elevons and rudders.

the flight actuators perfectly executed all the commands during the flight, which shows that no contamination was present in the system.

Planning for 'no-servicing requirements at launch pad' to minimize vehicle occupancy time

The actuation system was a complex one spread over the entire length and breadth of the vehicle. For such a system, one would naturally expect that a lot of servicing operations like gas charging, flushing, de-aeration, oil filling, etc. would be required on the launch pad. However, the system was designed with such provisions that no servicing would be required on the launch pad. During the stage preparation, these operations were carried out in the nearby assembly building. The two stages were individually transported in oil-charged and pressurized condition to the launch pad. The hydraulic systems of the two stages were just coupled using QCDCs. Thus no servicing was required for the actuation system at the launch pad, and the vehicle occupancy time at the launch pad could be greatly reduced.

Validation

Pre-launch tests: qualification and acceptance tests

All the control components and the actuation system were subjected to a rigorous formal qualification test programme to prescribed tests and levels. The following list gives an overview of the qualification tests. The list is not exhaustive. (a) Structural integrity tests (like proof pressure, burst pressure tests, over-tightening torque tests, repeated assembly tests, etc.). (b) Stress performance tests. (c) Environmental tests (compatibility tests, accelerated

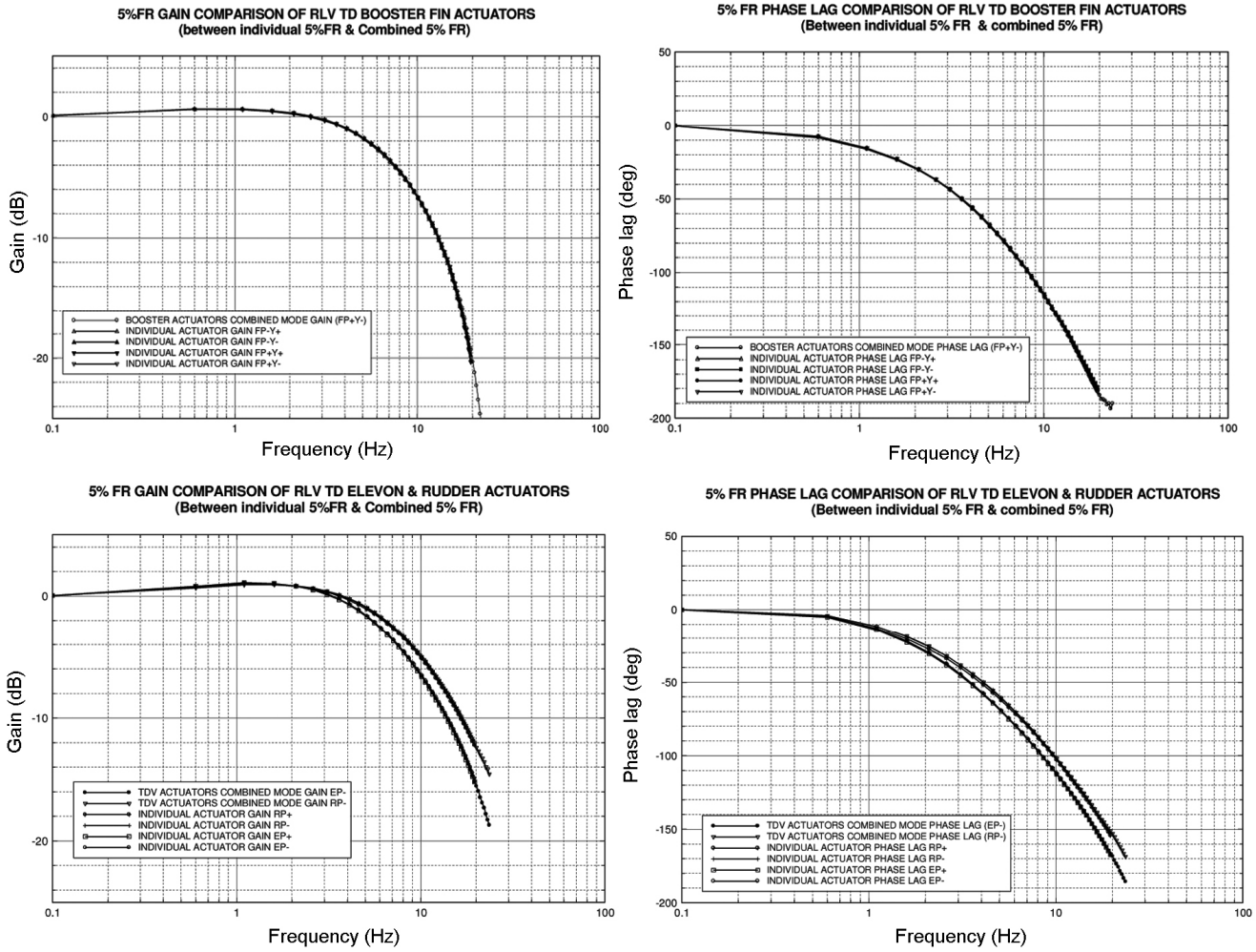

Figure 29. Performance of the actuation system as an integral system during 5% frequency response tests on Iron Bird test rig.

ageing tests, vibration tests, shock tests, humidity tests, hot soak, cold soak, EMI tests, EMC tests, acoustic tests, etc). Figure 25 shows the qualification vibration testing of actuators. (d) Endurance tests. (e) Tap tests to assess natural frequencies. (f) Stall force tests. (g) Impact load tests. (h) Electrical checks.

Similarly, all the control components and the actuation system identified for flight were subjected to extensive laboratory-level acceptance testing. The dynamically varying aerodynamic loads could not be simulated in the laboratory. Attempts to simulate the dynamically varying aerodynamic load would consume unaffordable time and cost disproportionate to the project cost. Therefore, the actuators and the system were tested under no load. By design, as is the common practice, it was ensured that the 'load–velocity curve (load locus)' of each of the eight actuators was lying well within the 'load-flow capability curve' of the servo valve (i.e. with adequate margin). This would ensure that the load pressure available at the maximum load velocity is more than adequate to move the specified maximum load at specified slew rates. As a confirmatory measure, one actuator was subjected to various tests (like frequency response, step response, ramp response, etc.) on a mechatronic test rig using an opposing loading actuator applying a constant load on the test actuator. This test confirmed that there was no difference between the no-load performance and performance under load of the actuator.

Iron Bird test rig for actuator in loop simulation tests

The full actuation system with all its elements: Li-ion battery, BLDC motor controller, BLDC motor, pump, check valve, accumulator, reservoir, filters, all actuators, plumbing lines, manifolds, etc. was mounted on an exclusively developed Iron Bird test rig. As an integral system, extensive validation was carried out by simulation experts during several rounds of flight simulation (ALS) using this test rig. Initially, proto model of the actuation

system underwent several rounds of ALS. The flight hardware was also subjected to minimal nominal ALS runs in the test rig and thus ruggedness was ensured. Figure 26 shows the second stage portion Iron Bird test rig of the vehicle. Figures 27 and 28 show the results of ALS runs. In Figure 29, the performance of the integrated system during 5% frequency response (FR) tests (i.e. when all the four actuators of each stage were simultaneously commanded) is compared with that of the actuators when they are individually tested. During this test, all the four actuators of each stage were simultaneously commanded. However, due to data acquisition limitation, response from one actuator only was acquired during this test and the response compared with the test results of 5% FR individual tests on all the four actuators. The performance of the system was normal and bandwidth specification was met by each of the eight actuators during the simultaneous 5% FR test.

Limitations in Iron Bird test rig for actuator in loop simulation tests

The following limitations were intentionally retained during validation of the actuation system in the Iron Bird test rig due to time and cost. However, alternate methods were adopted to evaluate their effects and it was ensured that they had no impact on the actuation system performance.

(a) Aerodynamic load and control surface inertia could not be simulated due to time and cost.

(b) Pyro-based disconnect-cum-sealing mechanism was substituted with solenoid actuated isolation valves for safety reasons and due to the requirement of multiple simulation runs.

(c) Effect of vehicle acceleration was not simulated.

(d) Mounting stiffness of the actuators was not exactly simulated.

(e) Flexibility of the vehicle was not simulated.

Performance of the actuation system during pre-flight tests

All the components and system identified for flight performed exceptionally well during all acceptance tests. Figures 24, 30, 31 show plots of few such tests carried out. Many more tests like vehicle-level sign checks, umbilical pull-out test, slow sine checks, and the effect of BLDC motor running on other co-existing systems were conducted at full vehicle level.

Performance of the centralized power plant-driven electrohydraulic control actuation system in the RLV-TD HEX-01 mission on 23 May 2016

The first ever centralized power plant-driven electrohydraulic control actuation system with eight actuators and a complex network of control components and plumbing performed exceptionally well in the RLV-TD HEX-01 mission. Many new technologies adopted in this actuation system were flight-proven. An overview of the performance of the actuation system in the mission is given below. Figures 21, 32 and 33 show the corresponding plots.

- For all fin, elevon and rudder actuators, feedbacks followed the commands.
- Maximum load on actuator was 18.6% of the stall force capability and 27.9% of the peak dynamic force capability.
- Oil temperature rise (ΔT) at the end of the mission was 22°C.

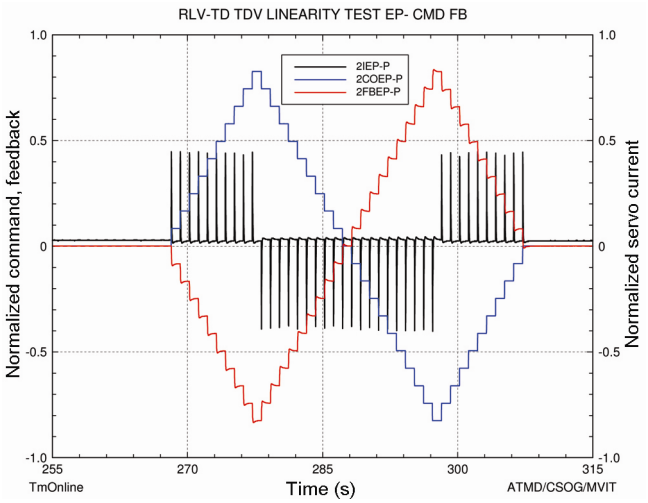

Figure 30. Results of linearity tests on second-stage actuators in full vehicle.

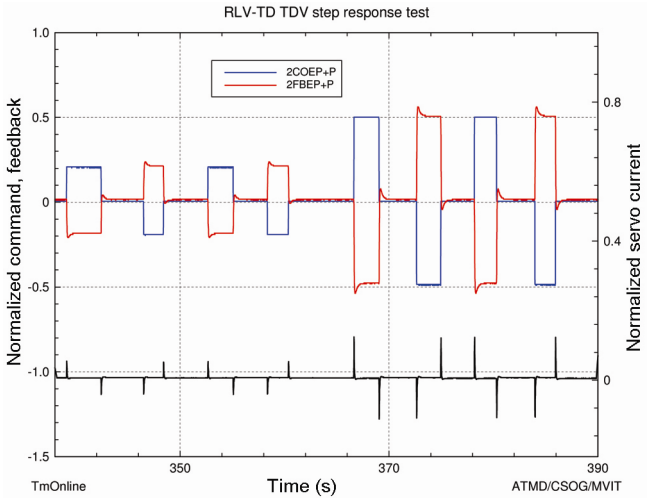

Figure 31. Results of step response tests on second-stage actuators in full vehicle.

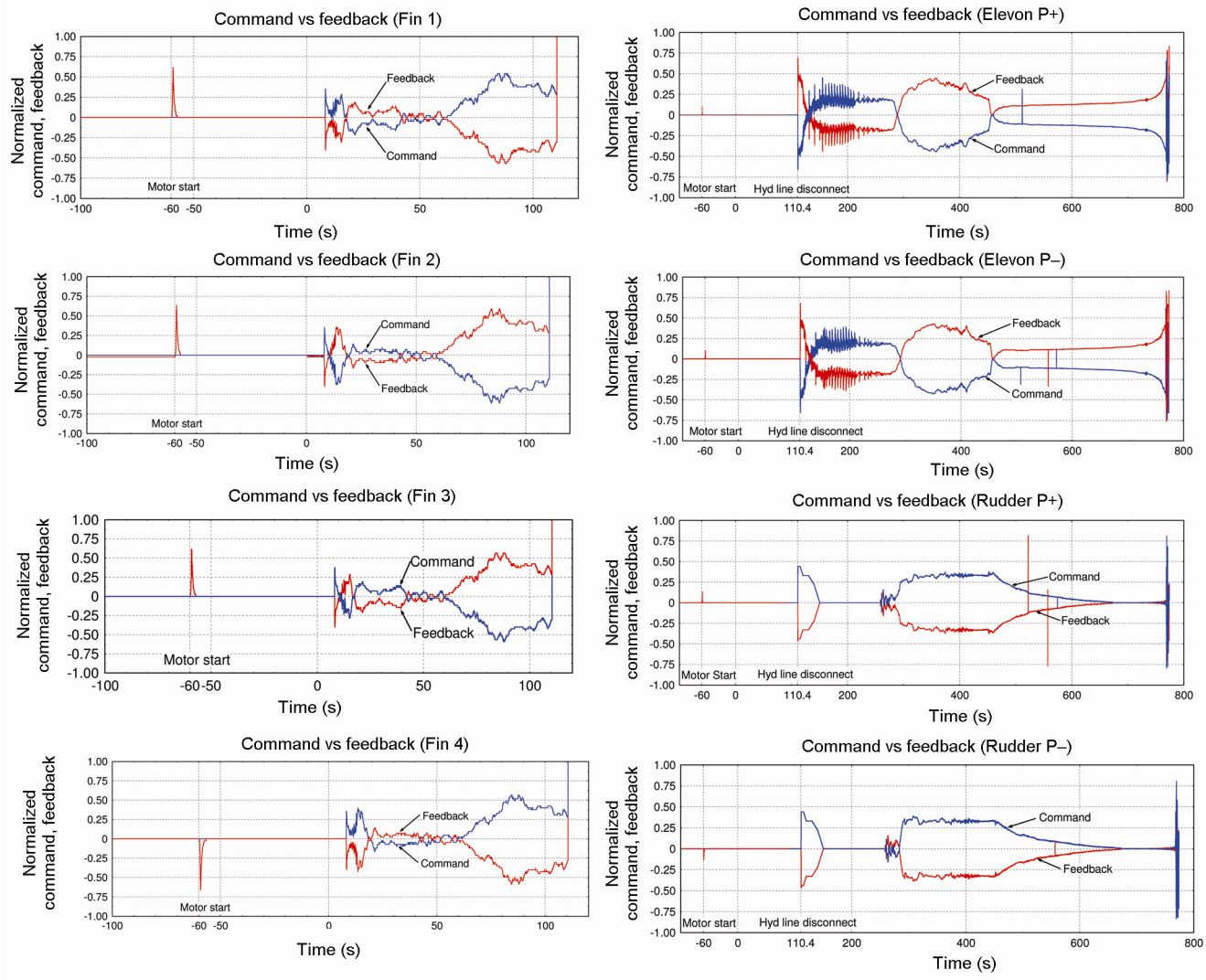

Figure 32. Performances of the actuators during the mission.

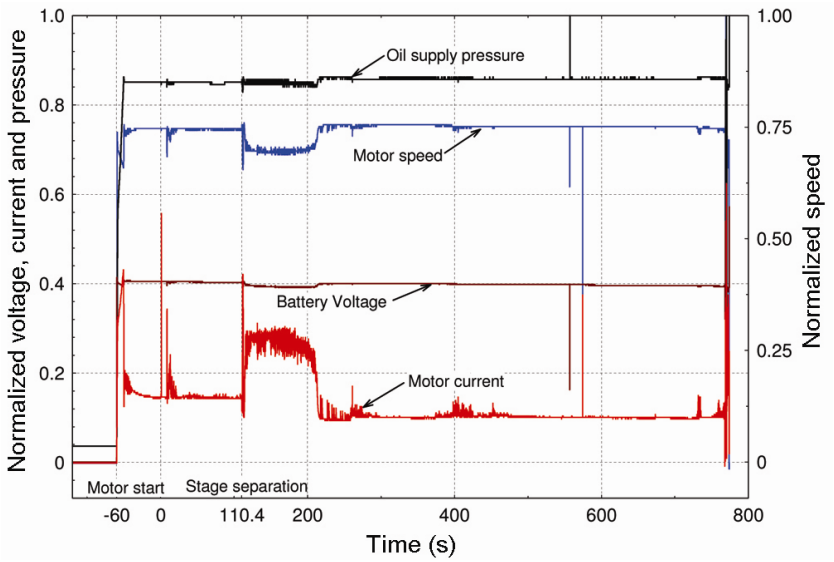

Figure 33. Performance of the power plant during the mission.

- Servo loop and control electronics performance was normal.
- BLDC motor performance was normal. The speed variation was within 800 RPM, matching with the variation of load on the motor.

Conclusion

A centralized power plant-driven electrohydraulic control actuation system with eight actuators and a complex network of control components and plumbing was successfully developed for the two-stage RLV-TD. The system was successfully qualified, evaluated in the Iron Bird test facility and flight-proven in the RLV-TD HEX-01 experimental mission on 23 May 2016. This mission proved the following with respect to the centralized power plant-driven electrohydraulic actuation system:

(a) Effectiveness of a centralized control power plant supplying hydraulic power to multiple actuators for vectoring multiple control surfaces.
(b) Effectiveness of single control power plant for attitude controlling multiple stages of a launch vehicle.
(c) Effectiveness of the power optimization strategies in minimizing the CPP power requirement.
(d) Pyro-based hydraulic line disconnect-cum-sealing scheme for disconnecting and sealing control actuation system hydraulic lines before stage-separation.
(e) Effectiveness of the thermal issues management strategies for a complex electrohydraulic control actuation system.
(f) Effectiveness of the contamination control and aeration control strategies for a complex aerospace hydraulic actuation system.
(g) Effectiveness of flexibility provisions for hydraulic plumbing lines and pressure vessels.

1. Merritt, H. E., *Hydraulic Control Systems*, John Wiley, New York, USA, 1967.

ACKNOWLEDGEMENTS. We thank all those who provided support for the centralized power plant-driven electrohydraulic control actuation system for the successful RLV-TD HEX-01 mission on 23 May 2016. We also thank the authorities of the Indian Space Research Organization for permission to publish this work.

doi: 10.18520/cs/v114/i01/84-100